

Dynamics of traffic flow with real-time traffic information

Yasushi Yokoya*

Japan Automobile Research Institute, 2530 Karima, Tsukuba, Ibaraki 305-0822, Japan

(Received 25 March 2003; revised manuscript received 29 September 2003; published 30 January 2004)

We studied dynamics of traffic flow with real-time information provided. Provision of the real-time traffic information based on advancements in telecommunication technology is expected to facilitate the efficient utilization of available road capacity. This system has a potentiality of not only engineering for road usage but also the science of complexity series. In the system, the information plays a role of feedback connecting microscopic and macroscopic phenomena beyond the hierarchical structure of statistical physics. In this paper, we tried to clarify how the information works in a network of traffic flow from the perspective of statistical physics. The dynamical feature of the traffic flow is abstracted by a contrastive study between the nonequilibrium statistical physics and a computer simulation based on cellular automaton. We found that the information disrupts the local equilibrium of traffic flow by a characteristic dissipation process due to interaction between the information and individual vehicles. The dissipative structure was observed in the time evolution of traffic flow driven far from equilibrium as a consequence of the breakdown of the local-equilibrium hypothesis.

DOI: 10.1103/PhysRevE.69.016121

PACS number(s): 05.70.Ln, 89.75.-k, 89.75.Fb, 05.65.+b

I. INTRODUCTION

Statistical physics is being applied to complex systems such as many-body problems outside the traditional domain of physical systems, e.g., biological and social sciences. In these applications, vehicular traffic has been studied for almost half a century in order to understand its unique phenomena. Theoretical analysis and computer simulation from the perspective of statistical physics not only provide fundamental aspects, but also support a better understanding of the complex phenomena observed in real traffic [1–3]. Furthermore, it is worthy of attention that these benefits in the study of vehicular traffic offer the possibility of understanding the various fundamental aspects of dynamics of truly nonequilibrium systems. In this paper, we study dynamics of traffic flow with information provided, which brings about a different kind of aspect in statistical physics.

Statistical physics provides us two main—but different—concepts for modeling vehicular traffic as a nonequilibrium system. One is a macroscopic approach based on a fluid-dynamical description. In this framework, traffic is viewed as compressible fluid formed by vehicles that do not appear explicitly [4–6]. The other concept is a microscopic approach, where each vehicle is represented by interacting particles [7–15]. We can generally distinguish these frameworks from their characteristic scales in space and time. For example, the characteristic scale in the fluid-dynamical description corresponds to the wavelength (or frequency) of compression waves driven in traffic flow. In contrast, the characteristic scale in the microscopic description is given by headway distance, which is interpreted as the mean free path determined in the traditional kinetic theory of gases. In general, the ratio of the characteristic scale plays the role of a small expansion parameter to distinguish different approaches as stated above, and gives us validity of approximation schemes of analytical calculation. A hierarchical

structure constructed by these characteristic scales is a useful concept in statistical physics for understanding complex natural phenomena.

This paper seeks to understand the dynamic relation between traffic flow and information from the perspective of statistical physics. This may provide interesting dynamics beyond the hierarchy in statistical physics, as well as a state driven far from equilibrium. Recently, increasing traffic congestion, especially in cities, underscores the importance of efficiently utilizing the available road capacity. Provision of real-time traffic information based on advancements in telecommunication technology is expected to improve the imbalance of traffic flow distribution in the road network. This system comprises three phases in real time: collection of observable quantities measured by roadside facilities, processing of collected data, and provision of traffic information. However, providing real-time information may have an adverse effect, such as causing over-reaction and concentration, even though it is meant to benefits such as to bring about efficient distribution of vehicles [16–21]. When real-time information is provided, a greater number of drivers will tend to concentrate on a recommended route, and consequently generate oscillations in road usage. As a result, the state of vehicular traffic is driven far from equilibrium, where a response feature of traffic flow based on many-body effects plays an important role.

To model traffic flow provided with real-time traffic information, it is essential to express the instantaneous circulation of information throughout the system. In the system, car-following behavior and route decision at an intersection are microscopic phenomena, spread throughout the whole state of traffic flow as macroscopic phenomena, e.g., average velocity through the medium of traffic information. This suggests that traffic information plays a role of feedback that connects the microscopic and the macroscopic phenomena beyond the hierarchical structure of statistical physics.

In order to study the dynamics of the system, we should first describe traffic flow by the microscopic framework that represents the interacting vehicles. There are mainly three

*Electronic address: yyokoya@jari.or.jp

different microscopic frameworks for modeling vehicular traffic: the kinetic theory, the car-following theory, and the particle-hopping theory.

In the kinetic theory, the probabilistic description of vehicular traffic is developed on the analogy of the kinetic theory of gases, where traffic is treated as gas of interacting particles [7–15]. In this framework, the time evolution of the distribution function of vehicles is given by the Boltzmann-like equation, where the correlation between a leading vehicle and a following one is almost negligible. Therefore, the one-particle distribution function is valid in a scale of the headway distance, namely, the mean free path.

In the car-following theory [22], a deterministic description of the motion of individual vehicles is provided by the principles of Newtonian dynamics. In this formulation, the potential energy between vehicles is originated by the stimulus every vehicle receives. The stimulus consists of the external force due to environment, e.g., geometry of a road, as well as the interaction with all the other vehicles in the system. In general, the stimulus can be expressed by the function of the speed of the vehicle, the difference in the speeds of the following vehicle and its leading one, the distance-headway, etc.

In the particle-hopping theory, traffic flow is described by the stochastic dynamics of individual vehicles, which is usually formulated by the cellular automata (CA) [23–26]. The CA model is ideal for an efficient large-scale computer simulation owing to discretization of position, speed, acceleration, and time. The discretization provides us not only computational efficiency but also an effective aspect of the dynamics of vehicular traffic, where a characteristic dissipation process of the car-following behavior is reduced to the hopping dynamics of particles on lattice sites. Moreover, the results of a computer simulation based on the CA model has been tried to compare with not only theoretical analysis (e.g., Burger’s equation interpreted by the ultradiscretization [27,28]), but also with empirical results from real vehicular traffic [29–37].

In this paper, we first study the dynamics of traffic flow under the provision of real-time information by means of the computer simulation based on the CA model. Next, we analyze the system theoretically from the perspective of non-equilibrium statistical physics. In the analysis, we apply the kinetic theory to the system. The results of the theoretical analysis are compared with those obtained from the computer simulations based on the CA model. In the above chain of analysis, we find that the computer simulation enables us to abstract characteristic features of the system as well as to examine validity of the approximation scheme of the analytical calculations.

This paper is organized as follows. Section II describes the equation of motion of traffic flow conforming to CA. Section III presents the time evolution of traffic flow. Section IV analyzes the time dependence of traffic flow from the perspective of nonequilibrium statistical physics. Finally, the paper concludes with Sec. V.

II. EQUATION OF MOTION

This section introduces an equation of motion of the CA that moves on a couple of single-lane crossings in one inter-

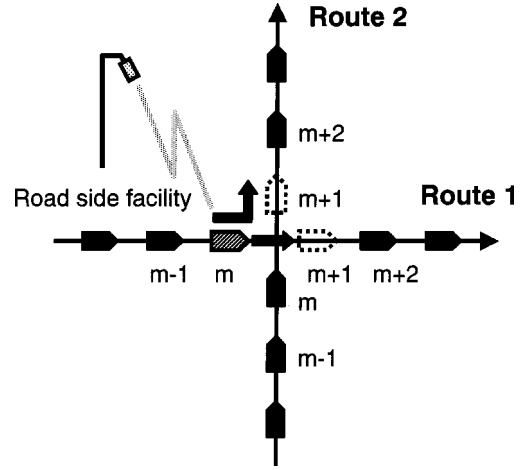


FIG. 1. An outline of the simulation model. At the intersection, each driver decides on a route from the information constantly provided by a road side facility.

section, as described in Fig. 1. Distribution of vehicles of an i th lattice site on route l ($l=1$ or 2) at time t is expressed by a binary array, ${}^l\mu_i(t) = \{0,1\}$. In the CA complying with the rule 184 [23], the variable takes on ${}^l\mu_i(t) = 0$ when a lattice site is empty and ${}^l\mu_i(t) = 1$ when a lattice site is occupied. At each discrete time step, $t \rightarrow t+1$, an arbitrary arrangement of vehicles is updated synchronously as follows:

$$X_i(t+1) = \begin{cases} M_i(t)Y_i(t) & \text{otherwise} \\ M_i(t)F_i(t) & \text{for } i=m \\ M_i(t)G_i(t) & \text{for } i=m+1. \end{cases} \quad (2.1)$$

The equation of motion in each route is given by a diagonal part of Eq. (2.1) as follows:

$$\begin{aligned} {}^1\mu_i(t) &= (X_i(t))_{11}, \\ {}^2\mu_i(t) &= (X_i(t))_{22}. \end{aligned} \quad (2.2)$$

The upper of the Eq. (2.1) represents the motion of CA, except for lattice sites around the intersection. The middle and lower of the Eq. (2.1) represent the motion of CA immediately before ($i=m$) and after ($i=m+1$) the intersection. The equations describe the behavior of drivers at an intersection in which drivers decide a route based on real-time traffic information, illustrated in Fig. 1.

The matrices on the right-hand side of Eq. (2.1) are given by the binary array ${}^l\mu_i(t)$ as follows:

$$M_i(t) = \begin{pmatrix} {}^1\mu_i(t) & \overline{{}^1\mu_i(t)} \\ {}^2\mu_i(t) & \overline{{}^2\mu_i(t)} \end{pmatrix}, \quad (2.3)$$

$$Y_i(t) = \begin{pmatrix} {}^1\mu_{i+1}(t) & {}^2\mu_{i+1}(t) \\ {}^1\mu_{i-1}(t) & {}^2\mu_{i-1}(t) \end{pmatrix}, \quad (2.4)$$

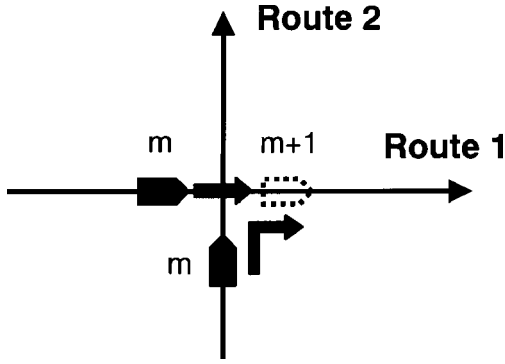


FIG. 2. The arrangement of vehicles in a concurrent occupancy case. Each vehicle advances at the probability 0.5.

$$F_i(t) = \begin{pmatrix} {}^1f_{i+1}(t) & {}^2f_{i+1}(t) \\ {}^1\mu_{i-1}(t) & {}^2\mu_{i-1}(t) \end{pmatrix}, \quad (2.5)$$

$$G_i(t) = \begin{pmatrix} {}^1\mu_{i+1}(t) & {}^2\mu_{i+1}(t) \\ {}^1g_{i-1}(t) & {}^2g_{i-1}(t) \end{pmatrix}, \quad (2.6)$$

$$\begin{aligned} {}^1f_i(t) &= {}^1\mu_i(t) {}^1\xi + {}^2\mu_i(t) \overline{{}^1\xi}, \\ {}^2f_i(t) &= {}^1\mu_i(t) \overline{{}^2\xi} + {}^2\mu_i(t) {}^2\xi, \\ {}^1g_i(t) &= {}^1\mu_i(t) {}^1\xi + {}^2\mu_i(t) \overline{{}^2\xi}, \\ {}^2g_i(t) &= {}^1\mu_i(t) \overline{{}^1\xi} + {}^2\mu_i(t) {}^2\xi. \end{aligned} \quad (2.7)$$

Here, $\overline{{}^l\mu_i(t)} = 1 - {}^l\mu_i(t)$ and $\overline{{}^l\xi} = 1 - {}^l\xi$. In the equations above, ${}^l\mu_{i+1}(t)$ [${}^l\mu_{i-1}(t)$] means distribution of an adjacent lattice site in the moving direction (opposite direction). Incidentally, calculations in the equations are dealt with according to the logical operation.

In Eq. (2.7), ${}^l\xi$ is a coefficient that determines whether the CA keeps or changes a route; the CA keeps a route for ${}^l\xi = 1$, and changes to another route for ${}^l\xi = 0$, as shown in Eq. (2.8).

$${}^l\xi = \begin{cases} 1 & \text{keep a route} \\ 0 & \text{change a route.} \end{cases} \quad (2.8)$$

The coefficient ${}^l\xi$ is decided by the traffic information. In this paper, we assume all drivers to be utilizing the traffic information provided at the intersection.

A word of caution is in order here. We permit only one vehicle to advance when two vehicles select the same lattice site at the intersection illustrated in Fig. 2. We give each of the two vehicles from different routes the same probability, 0.5, in order to avoid concurrent occupancy of a lattice site.

On each route with L lattice sites, CA has the following periodic boundary conditions:

$${}^l\mu_{L+1}(t) = {}^l\mu_1(t). \quad (2.9)$$

This therefore assures conservation of the total number of the CA on two routes.

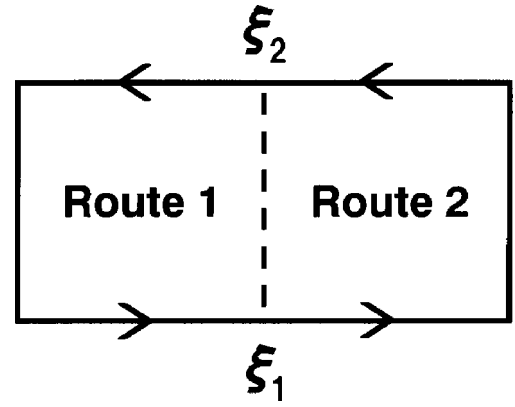


FIG. 3. A diagram of the simulation model. The broken line represents an intersection. Vehicles run following the arrows. At the intersection vehicles jump to another end of the broken line to keep their route while they pass the broken line to change their route.

The simulation model complying with Eqs. (2.1)–(2.9) can be described diagrammatically in Fig. 3, where the broken line represents an intersection and the arrows indicate a moving direction of vehicles. At the intersection vehicles jump to another end of the broken line to keep their route while they pass the broken line to change their route.

Before concluding this section, we would like to introduce some quantities observed in the system. Average velocity $\bar{v}_l(t)$ is defined as

$$\bar{v}_l(t) = \frac{n_l^a(t)}{n_l(t)}, \quad (2.10)$$

where $n_l^a(t)$ is the number of vehicles that advance at t , and $n_l(t)$ is the total number of vehicles on the route l . The vehicle density on route l is defined as

$$\rho_l(t) = \frac{n_l(t)}{L_l}, \quad (2.11)$$

where L_l is the number of lattice sites on route l . In the simulation, we adopted the size of the two routes as $L_1 = L_2 = L$ ($L = 500$).

III. SIMULATION OF RELAXATION PROCESS

In this section, we simulated traffic flow with real-time information provided. We adopted the information consisting of average velocity. For comparison, we also studied the traffic flow when a driver decided on a route randomly without any information. In the following simulation, we show the time dependence of average velocity and that of vehicle density on each route.

A. Provision of average velocity information

To provide real-time information based on average velocity, the coefficient at time t , ${}^l\xi_{\bar{v}}(t)$, is described by θ function as follows:

$${}^l\xi_{\bar{v}}(t) = \theta[\bar{v}_l(t) - \bar{v}_l(t)]. \quad (3.1)$$

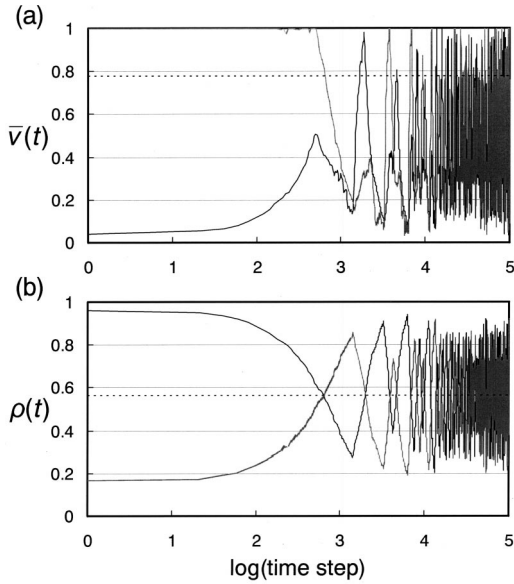


FIG. 4. Time dependence of average velocity (a) and vehicle density (b) on each route with real-time information provided. The initial density of vehicles on each route is 0.166 and 0.960. The broken lines represent the average velocity and the vehicle density in equilibrium state: $\bar{v}_{eq}=0.776$, $\rho_{tot}=0.563$. The log is to the base 10.

This equation indicates that a driver selects a route l when the average velocity exceeds that of another route l' .

Figures 4(a) and 4(b) illustrate the time dependence of average velocity $\bar{v}_l(t)$ and that of vehicle density $\rho_l(t)$ for an initial vehicle density in each route of $\rho_1=0.166$ and $\rho_2=0.960$. In these figures, the broken line represents an equilibrium distribution of vehicles, with $\bar{v}_{eq}=0.776$ at $\rho_{tot}=0.563$, which is given by the following equation:

$$\bar{v}_{eq} = \begin{cases} 1, & 0 \leq \rho_{tot} \leq 0.5, \\ \frac{1 - \rho_{tot}}{\rho_{tot}}, & 0.5 \leq \rho_{tot} \leq 1. \end{cases} \quad (3.2)$$

Here, the total vehicle density ρ_{tot} is given as follows:

$$\rho_{tot} = \frac{\sum_{l=1,2} n_l}{\sum_{l=1,2} L_l}. \quad (3.3)$$

Equation (3.2) represents the phase transition from free flow to congestion flow when the system is half-filled, $\rho_{tot}=0.5$.

The broken line represents the total vehicle density ρ_{tot} in Fig. 4 (b). We found chaotic oscillation in the simulation results of $\bar{v}_l(t)$ and $\rho_l(t)$. The complex structures in the time evolution, $\bar{v}_l(t)$ and $\rho_l(t)$, are caused by a concentration of vehicles that rush for a route recommended by the traffic information. The average velocity $\bar{v}_l(t)$ continues to vibrate with large amplitude and does not appear to converge, even for an intermediate density of vehicles ($\rho_{tot}=0.563$). In par-

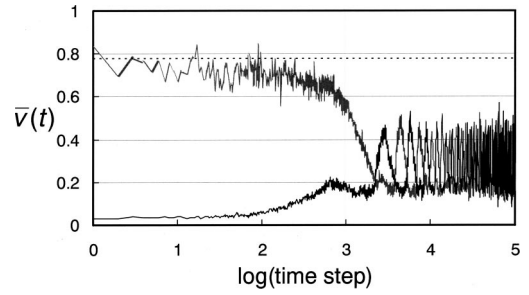


FIG. 5. Time dependence of average velocity on each route for $q=0.2$ with real-time information provided. The initial density of vehicles on each route is 0.166 and 0.960. The broken line represents the average velocity in equilibrium state: $\bar{v}_{eq}=0.776$.

ticular, we can confirm in the result of $\rho_l(t)$ [Fig. 4(b)] that the vehicle density in each route overshoots the equilibrium given at $\rho_{tot}=0.563$, and continues to oscillate just around ρ_{tot} with opposite phases.

Having described the results of a simulation based on the CA rule 184, let us now look at additional factors characterizing the dynamics of traffic flow, namely, randomness or noise effect of individual vehicles. The CA rule 184 adopted in the simulation is a minimal model for traffic flow. In addition, we can point out the importance of the different behaviors of individual drivers. Specifically, the effect corresponds to nondeterministic acceleration as well as overreaction while slowing down, which is crucially important for the spontaneous formation of traffic jams. Here we suppose that the speed of n th vehicle is decreased randomly by unity with probability q . The equation of motion under the supposition is given as follows:

$$\mu_i(t+1) = r_i \mu_i(t) + \bar{r}_i \{ \mu_i(t) \mu_{i+1}(t) + \overline{\mu_i(t) \mu_{i-1}(t)} \}, \quad (3.4)$$

here, $\bar{r}_i = 1 - r_i$ and

$$r_i = \begin{cases} 1 & \text{for probability } q \\ 0 & \text{for probability } 1 - q \end{cases} \quad (0 \leq q \leq 1). \quad (3.5)$$

In Eq. (3.5), the probability distribution is given by the uniform pseudorandom number due to the linear congruential method. Note that the limit case of $q=0$, namely, without the effect of randomness or noise, has been already shown in Fig. 4. On the other hand, it has been confirmed that traffic flow turns out to vanish in the limit case of $q=1$ in the stationary state irrespective of the vehicle density. In the actual traffic, the value of q can spread widely according to different driver temperaments and traffic conditions, etc. In Fig. 5, we show simulation results of time evolution of the average velocity for $q=0.2$. In this figure, we can find that the effect of randomness or noise tends to suppress the complex structures. Note that the average velocity in equilibrium is diminished by the effect.

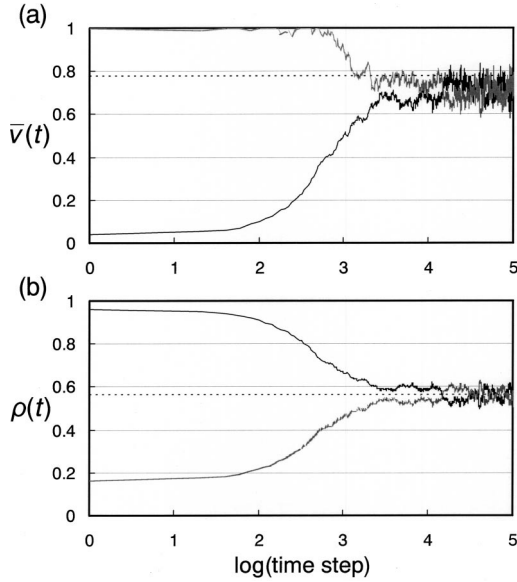


FIG. 6. Time dependence of average velocity (a) and vehicle density (b) on each route without provision of information where drivers select a route randomly. The initial density of vehicles on each route is 0.166 and 0.960. The broken lines represent the average velocity and the density of vehicles in equilibrium state: $\bar{v}_{\text{eq}} = 0.776$, $\rho_{\text{tot}} = 0.563$.

B. Random route decision (without information)

In this section, we simulate traffic flow without any information in order to contrast with that when real-time information is provided. When a driver selects a route without any information, we assume a driver determines a route randomly. The coefficient ${}^l\xi_R(t)$ is described as follows:

$${}^l\xi_R(t) = \begin{cases} 1 & \text{for probability } p \\ 0 & \text{for probability } 1-p \end{cases} \quad (0 \leq p \leq 1), \quad (3.6)$$

here, the probability distribution is given by the same way in Eq. (3.5).

Figures 6(a) and 6(b) present the time dependence of average velocity $\bar{v}_l(t)$ and of vehicle density $\rho_l(t)$ where the initial vehicle densities of the routes are $\rho_1 = 0.166$ and $\rho_2 = 0.960$. In this simulation, we adopt $p = 0.5$, where the driver selects either route impartially. We find that traffic flow imbalance between the routes is gradually relaxed, in contrast to the results of providing information shown in Fig. 4. Moreover, in the evolution curves of $\bar{v}_l(t)$ and $\rho_l(t)$, we can observe fluctuation near the equilibrium at $\rho_{\text{tot}} = 0.563$.

The above is a simulation for $p = 0.5$, let us now examine other cases of different probability p . Each vehicle in the system tends to change (keep) its own route for $p < 0.5$ ($p > 0.5$). As a result, relaxation of a gradient of vehicle density between two routes is accelerated (decelerated) for $p < 0.5$ ($p > 0.5$). In actual vehicular traffic, a value of p is closely related to not only driver temperaments and driving habits but also traffic conditions around the intersection. For example, the case of p close to zero seems to be relevant to

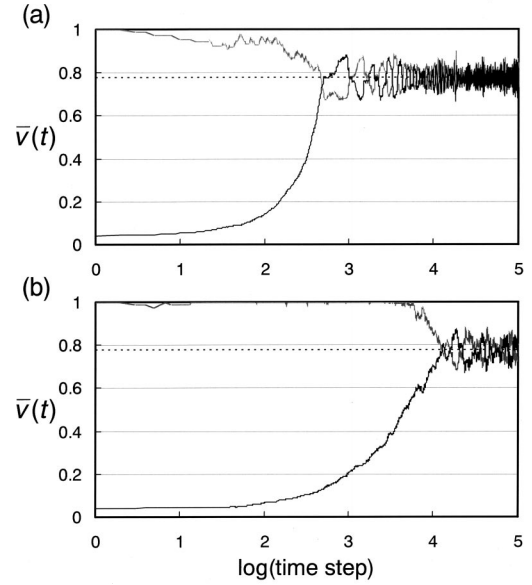


FIG. 7. Time dependence of average velocity on each route without provision of information where drivers select a route at the probability: (a) $p = 0.1$, (b) $p = 0.9$. The initial density of vehicles on each route is 0.166 and 0.960. The broken lines represent the average velocity and the density of vehicles for equilibrium state: $\bar{v}_{\text{eq}} = 0.776$, $\rho_{\text{tot}} = 0.563$.

the situation where drivers react individually on the traffic information, e.g., a local radio station. In Fig. 7, we show two extreme simulation results for $p = 0.1, 0.9$.

IV. DISSIPATIVE STRUCTURE OF TRAFFIC FLOW

In the preceding section we showed that real-time information resulted in spontaneous oscillation in the time evolution of traffic flow. Let us now turn our attention to the cause of the oscillation in traffic flow when real-time information is provided. For this section, we studied the traffic flow from the kinetic theory of gases.

We can characterize vehicular traffic by its wide range of density. In fact, vehicular traffic density ranges from quite low in which a vehicle runs almost freely to high (a traffic jam). In order to define the thermodynamic quantities of vehicular traffic, we must confirm whether or not the local-equilibrium hypothesis is fulfilled in the system. In general, the system realizes the local equilibrium by dissipation, with a sufficient number of particle collisions. Therefore in traffic flow, we may not be able to assume a local equilibrium in quite low density with few instances of interaction between vehicles. Fortunately, a unique dissipation process due to the driver's optimal velocity and the speed limit makes it possible to assume the conditions of the local equilibrium without a sufficient number of "collisions" in traffic flow. Parenthetically, we note that CA rule 184 adopted in the simulation can be regarded as the most naive model for realizing the unique dissipation process in vehicular traffic.

In this section, we define the thermodynamic quantity of traffic flow based on the mechanism of the dissipation process stated above.

A. Production and application of entropy

For a one-dimensional traffic flow, we can introduce the following statistical quantity:

$$H_l(t) = \int \int dv dx f_l(x, v, t) \ln f_l(x, v, t), \quad (4.1)$$

where f_l denotes the one-body distribution function of a route, l denotes position, x represents velocity v at time t . Furthermore, f_l satisfies the normalization relation as follows:

$$\int \int dv dx f_l(x, v, t) = \rho_l(t). \quad (4.2)$$

The time evolution of f_l is described by the following equation, namely, the Boltzmann equation of traffic flow:

$$\frac{\partial f_l(x, v, t)}{\partial t} + v \frac{\partial f_l(x, v, t)}{\partial x} = \left(\frac{\partial f_l(x, v, t)}{\partial t} \right)_{\text{coll}}. \quad (4.3)$$

The left-hand side of the equation represents the time evolution for f_l without interaction, and the right-hand side represents the rate of change of f_l with time, due to interaction between vehicles, which corresponds to mutual collision of molecules in gases. The kinetic theory of vehicular traffic analogous to the Boltzmann equation was already introduced by modifying the concepts of gases [7–15].

We adopted a quite simple interaction based on CA rule 184 for single-lane traffic with the periodic boundary condition. The equation of motion of vehicles obeying the CA-184 rules is

$$\mu_i(t+1) = \mu_i(t)\mu_{i+1}(t) + \overline{\mu_i(t)\mu_{i-1}(t)}. \quad (4.4)$$

The above equation indicates that there are only two modes, $v=0$ and $v=1$. The state of $v=0$ is given by the interaction between vehicles that arises only when $\mu_i(t)=1$ and $\mu_{i+1}(t)=1$, while the state of $v=1$ is given for the other cases. The probability of a vehicle with $v=0$ at the route l is given by n_{0l} ($0 \leq n_{0l} \leq 1$) and that with $v=1$ is given by $1 - n_{0l}$. By means of the normalization relation given by Eq. (4.2) and the periodic boundary condition, a rate of change of H_l , with time is calculated as follows:

$$\frac{dH_l(t)}{dt} = \int \int dx dv \frac{\partial f_l(x, v, t)}{\partial t} \ln f_l(x, v, t) \quad (4.5)$$

$$= \rho_l \frac{dn_{0l}}{dt} \ln \left(\frac{n_{0l}}{1 - n_{0l}} \right). \quad (4.6)$$

In the last equation, the space uniformity of f_l is assumed. When the probability n_{0l} is high, i.e., $n_{0l} > 0.5$, n_{0l} can be considered as a decreasing function of time based on the relaxation process due to the mutual collision of vehicles. On the other hand, n_{0l} is regarded to be constant with time when n_{0l} is small, i.e., $n_{0l} < 0.5$, where vehicles rarely encounter other vehicles. Therefore, it is possible to consider H_l as a

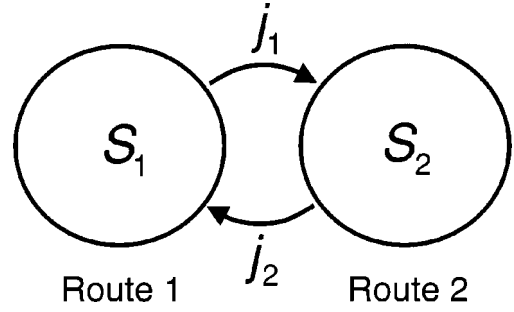


FIG. 8. The irreversible flow driven by the gradient of the entropy.

decreasing function of time. Based on the above consideration, we adopt H_l as the entropy of traffic flow that obeys the CA-184 rules as follows:

$$S_l(t) = -H_l(t) \quad (4.7)$$

$$= -\rho_l n_{0l} \ln n_{0l} - \rho_l (1 - n_{0l}) \ln (1 - n_{0l}). \quad (4.8)$$

Note that the ground state of the CA rule 184 is obtained exactly by its density given as follows [38,39]:

$$n_{0l} = 1 - \bar{v}_{\text{eq}} = \frac{2\rho_l - 1}{\rho_l}. \quad (4.9)$$

Having described the entropy of traffic flow, let us now consider the irreversible flow driven by a difference of the entropy in each route (Fig. 8).

Entropy production is a useful thermodynamic quantity for treating an irreversible flow [40–42]. The entropy production P is given as follows:

$$P = \int dV \sum_k J_k X_k. \quad (4.10)$$

In Eq. (4.10), V represents system volume and J_k the irreversible part of flow driven by the gradient of the intensive variable X_k ; k is an index of a constituent of a system, i.e., the pair of routes in which the irreversible flow is brought about. P is always restricted to $P \geq 0$ according to the second law of thermodynamics. The relation of $P=0$ and $P>0$ is given for both the reversible and irreversible processes. In general, P is bound to minimize itself in the steady state under some constraint, e.g., the boundary conditions of a system. The gradient of the intensive variable X_k corresponds to the differential coefficient of the entropy with respect to conservative quantities. We adopted the number of vehicles as the conservative quantity of a system. In traffic phenomena, the kinetic energy of vehicles dissipates to the internal energy of a system, e.g., combustion of fuel, radiation of heat from brakes, etc. As a result, the differential coefficient of the entropy with respect to density of vehicles is given as follows:

$$\frac{dS_l}{d\rho_l} = \left(\rho_l \frac{dn_{0l}}{d\rho_l} + n_{0l} \right) \ln \left(\frac{1 - n_{0l}}{n_{0l}} \right) - \ln(1 - n_{0l}). \quad (4.11)$$

We can find a component inversely proportional to ρ_l in the first and the second term of the right-hand side of Eq. (4.11), under the local-equilibrium hypothesis, i.e., $n_{0l} = 1 - \bar{v}_{\text{eq}} = (2\rho_l - 1)/\rho_l$. Therefore, it is reasonable to adopt $1/\rho_l$ as the intensive variable.

Based on the above consideration, we can express the gradient of the intensive variable X , between two routes, as follows:

$$X = \frac{1}{\rho_1} - \frac{1}{\rho_2}. \quad (4.12)$$

Incidentally, we can transform Eq. (4.12) into an expression with the average velocity in each route under the local-equilibrium hypothesis, which is given by Eq. (4.13),

$$X = \bar{v}_1 - \bar{v}_2. \quad (4.13)$$

The intensive variable described above corresponds to that of traffic flow when real-time information is provided, as mentioned later.

B. Diffusion process without information

In this section, we study the relaxation process of traffic flow without any information. In the system, an irreversible flow is driven by the difference in vehicle densities between routes. We will examine the time evolution of entropy production from analytical and numerical calculation approaches to determine the dynamic features of the system.

In order to describe the dynamics of traffic flow, we introduce the conservation equations of the number of vehicles without information in Eq. (4.14). In the following equations, the coefficients $1/L_1 = 1/L_2 = 1/L$ are omitted.

$$\begin{aligned} \frac{d\rho_1}{dt} &= \gamma \left(\frac{1}{\rho_1} - \frac{1}{\rho_2} \right) + R(t), \\ \frac{d\rho_2}{dt} &= \gamma \left(\frac{1}{\rho_2} - \frac{1}{\rho_1} \right) - R(t). \end{aligned} \quad (4.14)$$

Here, γ is a constant coefficient. In these equations, the equilibrium states of traffic flow are given at $\rho_1 = \rho_2$. The first term on the right-hand side of the equations corresponds to the phenomenological relations, e.g., Fick's law for diffusion. The second term on the right-hand side, $R(t)$, is the stochastic function expressed by a binary array, $R(t) = \{-\epsilon, \epsilon\}$, where $|\epsilon| \approx O(L^{-1})$; $R(t)$ represents random movement of vehicles between routes. Hence, the first term for the diffusion effect dominates over the dynamics of the system far from equilibrium, while the second term for randomness of vehicular movement becomes dominant near equilibrium. In general, it is useful to examine the system stability in order to understand the structure of the dynamics. Unfortunately, it is impossible to determine the stability of the system by linearization of these equations due to the structural instability at equilibrium. Therefore, we concentrated on calculating the entropy production in order to examine the system stability.

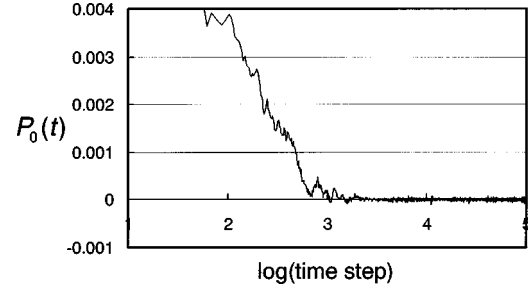


FIG. 9. Time dependence of the entropy production of traffic flow without information. The initial density of vehicles on each route is 0.166 and 0.960.

The system entropy production P_0 and its differentiation with respect to time, dP_0/dt , are given below

$$P_0 = \left(\frac{d\rho_1}{dt} - \frac{d\rho_2}{dt} \right) \left(\frac{1}{\rho_1} - \frac{1}{\rho_2} \right), \quad (4.15)$$

$$\begin{aligned} \frac{dP_0}{dt} &= \left(\frac{d^2\rho_1}{dt^2} - \frac{d^2\rho_2}{dt^2} \right) \left(\frac{1}{\rho_1} - \frac{1}{\rho_2} \right) \\ &+ \left(\frac{d\rho_1}{dt} - \frac{d\rho_2}{dt} \right) \left(\frac{1}{\rho_2^2} \frac{d\rho_2}{dt} - \frac{1}{\rho_1^2} \frac{d\rho_1}{dt} \right). \end{aligned} \quad (4.16)$$

The second term on the right-hand side of Eq. (4.16) is always negative, but the first term can be both positive and negative. When the system is driven far from equilibrium, namely, $|\rho_1 - \rho_2| \gg |R(t)|$, we can get $dP_0/dt \leq 0$. For the state near equilibrium, namely, $|\rho_1 - \rho_2| \approx |R(t)|$, we can get $dP_0/dt \approx 0$. Consequently, these analyses based on the entropy production assure the stability of the system except around equilibrium.

Next, we simulate the time evolution of the entropy production in order to confirm the above analysis. Figure 9 shows the time evolution of P_0 for initial vehicle densities $\rho_1 = 0.166$ and $\rho_2 = 0.960$. We find that P_0 decreases monotonically with fine structures and fluctuates around $P_0 = 0$ due to random movement of vehicles between routes. On the whole, the simulation result is consistent with that of the analysis based on the conservation equations for the number of vehicles stated above. In general transport phenomenon, e.g., the diffusion process, the irreversible flow J is driven proportionally to the gradient of the intensive variable X near equilibrium, where the entropy production is minimized in its steady state. Therefore, we can regard the transport phenomena observed in the traffic flow without any information as an ordinary diffusion process.

Incidentally, we gave the probability p which determines the rate of the route change ξ_R given in Eq. (3.6). In the time evolution of a vehicle density $\rho(t)$ the relaxation of the gradient of $\rho(t)$ between two routes is accelerated (decelerated) for $p < 0.5$ ($p > 0.5$) where each vehicle tends to change (keep) its own route. It means that the probability p is closely related to the diffusion coefficient of the system. Note that in the small value of p , namely, the large diffusion case, insta-

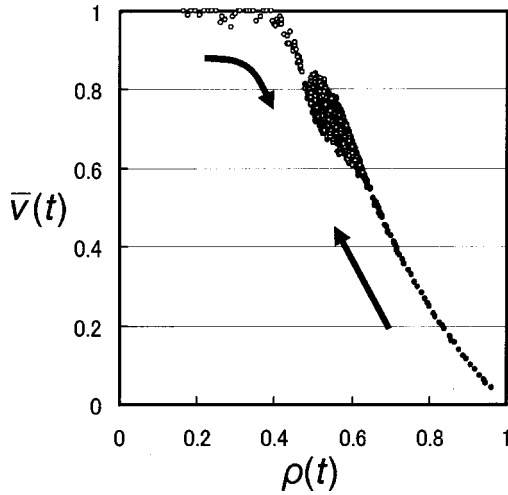


FIG. 10. The phase trajectory on $\bar{v}-\rho$ plane without information ($p=0.5$). The open circle and the solid one represent the trajectory in each route.

bility of the system with vibratory structures is induced by overshoot of traffic flow when the initial gradient of $\rho(t)$ between two routes is small.

Next, we attempt to confirm fulfillment of the local equilibrium in traffic flow, which is required to define the thermodynamic quantities of the system. We present a phase trajectory of traffic flow on $\bar{v}_l-\rho_l$ plane in Fig. 10. This figure indicates that the states of vehicular traffic in each route are distributed near equilibrium. This means that the scale of space (time) in variation of the states is sufficiently large in comparison with the mean free path (mean free time) of individual vehicles. We can therefore conclude that the states of traffic flow evolve with time under the local-equilibrium hypothesis.

C. Dissipation process with information provided

We now turn from the diffusion process in vehicular traffic without information and consider traffic flow dynamics when information is provided in real time. In the system, the irreversible flow is driven by the difference of average velocity in each route. In this section, we examine the dissipation of traffic flow when real-time information is provided.

First, we introduce the conservation equations of the number of vehicles when real-time information is provided as follows:

$$\begin{aligned} \frac{d\rho_1}{dt} &= \kappa\{\theta(\bar{v}_1 - \bar{v}_2) - \theta(\bar{v}_2 - \bar{v}_1)\}, \\ \frac{d\rho_2}{dt} &= \kappa\{\theta(\bar{v}_2 - \bar{v}_1) - \theta(\bar{v}_1 - \bar{v}_2)\}. \end{aligned} \quad (4.17)$$

Here, $\kappa(=1/L_1=1/L_2=1/L)$ is a constant. In these equations, equilibrium states are given at $\rho_1=\rho_2(\bar{v}_1=\bar{v}_2)$. Unfortunately, it is impossible to examine the stability of the system by linearization of these equations because of the

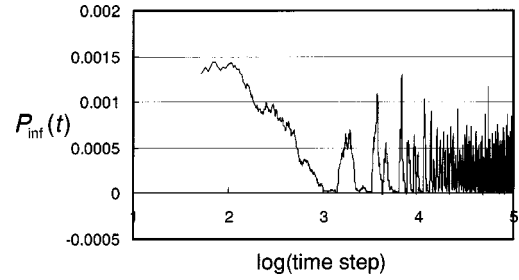


FIG. 11. Time dependence of the entropy production of traffic flow with real-time information provided. The initial density of vehicles on each route is 0.166 and 0.960.

structural instability at equilibrium. Therefore, we would like to examine the stability of the system by means of the entropy production.

In the system, vehicular traffic is expected to approach equilibrium by the irreversible traffic flow between routes, which is driven by the information based on average velocity. Therefore, the entropy production P_{inf} when information is provided is described by the gradient of the average velocity as follows:

$$P_{\text{inf}} = \left(\frac{d\rho_1}{dt} - \frac{d\rho_2}{dt} \right) (\bar{v}_1 - \bar{v}_2). \quad (4.18)$$

From the above equation, we can find that P_{inf} is the Lyapounov function. P_{inf} thus decreases monotonically with time as follows:

$$\begin{aligned} \frac{dP_{\text{inf}}}{dt} &= \left(\frac{d^2\rho_1}{dt^2} - \frac{d^2\rho_2}{dt^2} \right) (\bar{v}_1 - \bar{v}_2) \\ &\quad - \left(\frac{d\rho_1}{dt} - \frac{d\rho_2}{dt} \right) \left(\frac{d\bar{v}_1}{dt} - \frac{d\bar{v}_2}{dt} \right) \leq 0. \end{aligned} \quad (4.19)$$

This calculation presupposes that the average velocity in each route reaches its equilibrium value, namely, \bar{v}_{eq} given in Eq. (4.9). As a result, the analysis of P_{inf} based on the conservation equations of the number of vehicles ensures that the system is stable, as long as the local-equilibrium hypothesis is achieved at every moment in each route.

We can now simulate the time evolution of entropy production in order to confirm the above analysis. Figure 11 shows the time evolution of P_{inf} for initial vehicle density $\rho_1=0.166$ and $\rho_2=0.960$. In this figure, we find continuous and irregular vibratory structures driven far from equilibrium. The result suggests a breakdown of the local-equilibrium hypothesis. There is an inverse flow against the relaxation of the gradient of average velocity at a period, $dP_{\text{inf}}/dt > 0$, considering the structure of P_{inf} given in Eq. (4.18). To investigate this process, a phase trajectory of traffic flow on the $\bar{v}_l-\rho_l$ plane is plotted in Fig. 12. We find that the average velocity in each route is distributed far from equilibrium, and \bar{v}_l does not reach its equilibrium value \bar{v}_{eq} given in Eq. (4.9). These results indicate that the traffic information based on a nonequilibrium state is fed back into traffic flow at every moment. In the process, the state of

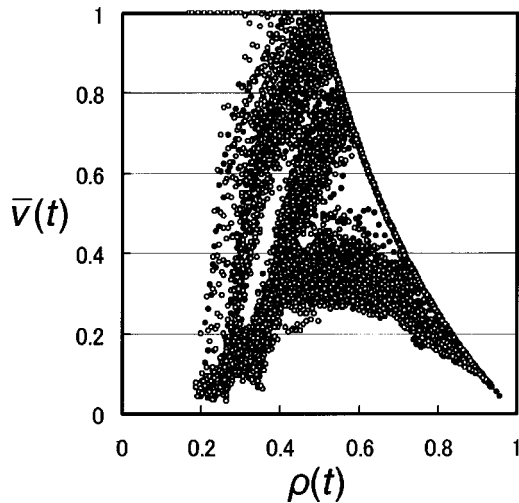


FIG. 12. The phase trajectory on \bar{v} - ρ plane with real-time information provided. The open circle and the solid one represent the trajectory in each route.

traffic in each route is spread instantaneously as traffic information before the state of traffic is relaxed by sufficient instances of vehicle interactions. In other words, the scale of space (time) for the variation of the state of traffic flow is comparable to the mean free path (mean free time) of individual vehicles. In this situation, the feedback process produces conflict between the average velocity and the density of vehicles, e.g., $\bar{v}_1 > \bar{v}_2$ does not necessarily give $\rho_1 < \rho_2$. As a result, the inverse flow against the gradient of the vehicle density is driven and causes complex vibratory structures in the time evolution of P_{inf} . It is remarkably different from the diffusion process of traffic flow without any information, where the local-equilibrium hypothesis in each route is satisfied at every moment.

In connection with the inverse flow against the gradient of the intensive variable, one should refer to the active transportation observed in the chemical reaction [42–44]. The active transportation is interpreted as a nonequilibrium process satisfying the local-equilibrium hypothesis, where the chemical reaction evolves more slowly than the relaxation of the system due to the elastic collision of particles. The active transportation in traffic flow with information provided originates from a breakdown of the local-equilibrium hypothesis, which is in contrast to that of the chemical reaction.

Before concluding this section, we should refer to the effect of randomness or noise of traffic flow given in Eqs. (3.4) and (3.5), on achievement of the local-equilibrium hypothesis. In Fig. 13, we show the time evolution of the entropy production, P_{inf} , considering the effect of randomness or noise with $q=0.2$, for initial vehicle densities $\rho_1=0.166$ and $\rho_2=0.960$. In this figure, we can find decrease of the vibratory structures. Moreover, in Fig. 14, it is shown a phase trajectory on \bar{v} - ρ plane for the same initial vehicle density. We can find structure such as the limit cycle around the equilibrium point, which is altered by the effect of randomness or noise. These results suggest restoration of the local-equilibrium hypothesis. We can consider that the restoration originates from the nondeterministic deceleration of an

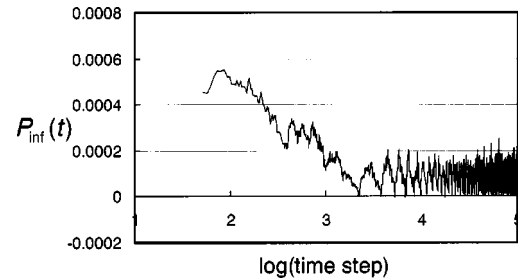


FIG. 13. Time dependence of the entropy production for $q=0.2$ with real-time information provided. The initial density of vehicles on each route is 0.166 and 0.960.

individual vehicle which increases instances of vehicle interactions, and furthers the relaxation of traffic flow.

V. CONCLUSION

In this paper we studied the dynamics of traffic flow when information was provided in real time. The dynamic feature of traffic flow was abstracted through the perspective of non-equilibrium statistical physics and the computer simulation based on CA.

For an imbalanced network of roads without any information, the irreversible traffic flow is driven proportionally to the gradient of the intense variable, namely, the inverse of the vehicle density. Therefore, the relaxation of traffic flow in a network of roads is interpreted as the diffusion process, where entropy production is minimized in the steady state. In the system, the local-equilibrium hypothesis is satisfied in each route; the scale of space (time) in variation of the state of traffic flow, i.e., the average velocity and the density of vehicles, is sufficiently large compared with the mean free path (mean free time) of individual vehicles.

Providing real-time information disrupts the local equilibrium of traffic flow in each route. In the system, the scale of space (time) in the variation of the state of traffic flow becomes comparable with the mean free path (mean free time)

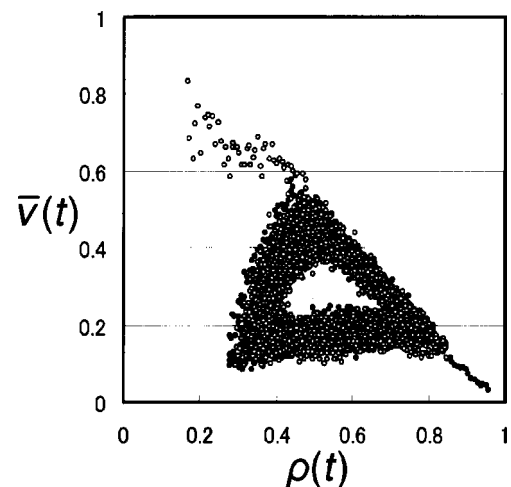


FIG. 14. The phase trajectory on \bar{v} - ρ plane for $q=0.2$ with real-time information provided. The open circle and the solid one represent the trajectory in each route.

of individual vehicles due to the instantaneous circulation of the state of traffic flow through a medium of information. The breakdown of the local-equilibrium hypothesis causes conflict in the relation between the average velocity and the vehicle density. This is the origin of the characteristic non-linear feedback of the system, by which backward flow is driven against the gradient of the vehicle density. As a result, complex structures of order, i.e., the dissipative structures, are created spontaneously, involving finite entropy production of traffic flow. Incidentally, the effect of randomness or noise in traffic flow works to restore the local-equilibrium hypothesis.

The contrastive study between the analysis from the perspective of statistical physics and the computer simulation based on CA revealed that the breakdown of the local-equilibrium hypothesis is essential in the dynamics of traffic flow with the provision of real-time information. For the system to work, it needs theoretical treatment of the dissipation flow, e.g., non-Fickian diffusion for the irreversible traffic flow between routes. Fortunately, there have already been several studies on the extended thermodynamics beyond the local-equilibrium hypothesis, where the irreversible process with a rapid change in space (time) disrupts the local equilibrium [45,46]. Furthermore, we can point out that the ASEP (asymmetric simple exclusion process) model has another potentiality of theoretical treatment of the system. The ASEP model is the simplest prototype of interacting systems driven

far from equilibrium, and one-dimensional model, in particular, is solved exactly [47,48]. In our model, therefore, it might be possible to utilize the exact treatment, e.g., the Bethe ansatz [49] and the free fermion, which succeeds in modeling one-dimensional spin or electron systems.

Finally, we refer to phase transitions of the system. The phase transitions in our model can be characterized by the provided information (contents, way of provision), topology of a network of roads with multi-intersections, and the boundary conditions, as well as vehicle density. In particular, the existence of so-called boundary-induced phase transitions have been demonstrated by computer simulations and exact calculations of the one-dimensional model with the open boundary conditions [47,50–52]. In these models, imbalance of insertion and removal of a vehicle at the boundary breaks the translational invariance and brings a variety of stationary states with a nontrivial density profile. It indicates that the boundary conditions play an important part in characterization of nonequilibrium systems. In our model, a combination of different boundary conditions in each route is expected to bring a variety of states.

ACKNOWLEDGMENT

The author wishes to thank T. Katayama for many helpful discussions and comments.

-
- [1] *Traffic and Granular Flow*, edited by D.E. Wolf, M. Schreckenberg, and A. Bachem (World Scientific, Singapore, 1996).
 - [2] *Traffic and Granular Flow '97*, edited by M. Schreckenberg and D.E. Wolf (Springer, Singapore, 1998).
 - [3] D. Chowdhury, L. Santen, and A. Schadschneider, *Phys. Rep.* **329**, 199 (2000).
 - [4] H. Greenberg, *Oper. Res.* **7**, 79 (1959).
 - [5] B.S. Kerner and P. Konhäuser, *Phys. Rev. E* **48**, R2335 (1993); **50**, 54 (1994).
 - [6] R.D. Kühne and R. Beckschulte, in *Proceedings of the 12th International Symposium on the Theory of Traffic Flow and Transportation*, edited by C.F. Daganzo (Elsevier Science, Berkeley, 1993), p. 367.
 - [7] I. Prigogine and F.C. Andrews, *Oper. Res.* **8**, 789 (1960).
 - [8] I. Prigogine, *Physica* **15**, 272 (1949).
 - [9] S.L. Paveri-Fontana, *Transp. Res.* **9**, 225 (1975).
 - [10] H. Lehmann, *Phys. Rev. E* **54**, 6058 (1996).
 - [11] T. Nagatani, *Physica A* **237**, 67 (1997); *J. Phys. Soc. Jpn.* **66**, 1219 (1997).
 - [12] C. Wagner, *Physica A* **245**, 124 (1997); *J. Stat. Phys.* **90**, 1251 (1998).
 - [13] C. Wagner, C. Hoffmann, R. Sollacher, J. Wagenhuber, and B. Schürmann, *Phys. Rev. E* **54**, 5073 (1996).
 - [14] D. Helbing, *Phys. Rev. E* **53**, 2366 (1996); **57**, 6176 (1997).
 - [15] D. Helbing and M. Treiber, *Phys. Rev. Lett.* **81**, 3042 (1998).
 - [16] T.L. Friesz, J. Luque, R.L. Tobin, and B.-W. Wie, *Oper. Res.* **37**, 893 (1989).
 - [17] M. Ben-Akiva, A. de Palma, and I. Kaysi, *Transp. Res., Part A* **25**, 251 (1991).
 - [18] H.S. Mahmassani and R. Jayakrishnan, *Transp. Res., Part A* **25**, 293 (1991).
 - [19] R. Arnott, A. de Palma, and R. Lindsey, *Transp. Res., Part A* **25**, 309 (1991).
 - [20] P. Kachroo and K. Özbay, *Transp. Res. Rec.* **1556**, 137 (1996).
 - [21] Y. Yokoya, in *Proceedings of the IEEE International Vehicle Electronics Conference*, edited by S. Washino (Tottori University of Environmental Studies, Tottori, Japan, 2001), p. 203.
 - [22] R.W. Rothery, in *Traffic Flow Theory*, edited by N. Gartner, C. J. Messner, and A.J. Rathi, Transportation Research Board (TRB) Special Report, Vol. 165 (Transportation Research Board, Washington, D.C., 1992), Chap. 4.
 - [23] S. Wolfram, *Rev. Mod. Phys.* **55**, 601 (1983).
 - [24] K. Nagel, J. Esser, and M. Rickert, in *Annual Reviews of Computational Physics*, edited by D. Stauffer (World Scientific, Singapore, 2000), p. 151.
 - [25] K. Nagel and M. Schreckenberg, *J. Phys. I* **2**, 2221 (1992).
 - [26] O. Biham, A.A. Middleton, and D. Levine, *Phys. Rev. A* **46**, R6124 (1992).
 - [27] T. Tokihiro, D. Takahashi, J. Matsukidaira, and J. Satsuma, *Phys. Rev. Lett.* **76**, 3247 (1996).
 - [28] K. Nishinari and D. Takahashi, *J. Phys. A* **31**, 5439 (1998); **32**, 93 (1999).
 - [29] S. Migowsky, T. Wanschura, and P. Ruján, *Z. Phys. B: Condens. Matter* **95**, 407 (1994).
 - [30] K. Nagel, D.E. Wolf, P. Wagner, and P. Simon, *Phys. Rev. E* **58**, 1425 (1998).
 - [31] P. Simon and K. Nagel, *Phys. Rev. E* **58**, 1286 (1998).
 - [32] J. Esser and M. Schreckenberg, *Int. J. Mod. Phys. C* **8**, 1025 (1997).

- [33] K. Nagel, *Int. J. Mod. Phys. C* **7**, 883 (1996).
- [34] K. Nagel, *Phys. Rev. E* **53**, 4655 (1996).
- [35] K. Nagel and C.L. Barrett, *Int. J. Mod. Phys. C* **8**, 505 (1997).
- [36] M. Rickert and P. Wagner, *Int. J. Mod. Phys. C* **7**, 133 (1996).
- [37] M. Rickert and K. Nagel, *Int. J. Mod. Phys. C* **8**, 483 (1997).
- [38] M. Schreckenberg, A. Schadschneider, K. Nagel, and N. Ito, *Phys. Rev. E* **51**, 2939 (1995).
- [39] A. Schadschneider and M. Schreckenberg, *J. Phys. A* **26**, L679 (1993).
- [40] P. Gransdorff and I. Prigogine, *Thermodynamic Theory of Structure, Stability and Fluctuations* (Wiley-Interscience, London, 1971).
- [41] J.S. Kirkaldy, *Phys. Rev. A* **31**, 3376 (1985).
- [42] G. Nicolis and I. Prigogine, *Self-Organization in Nonequilibrium Systems* (Wiley, New York, 1977).
- [43] O.K. Wilby and G. Webster, *J. Embryol. Exp. Morphol.* **24**, 583 (1970).
- [44] P.A. Lawrence, *J. Exp. Biol.* **44**, 607 (1966).
- [45] D. Jou, J. Casas-Vasquez, and G. Lebon, *Extended Irreversible Thermodynamics*, 3rd ed. (Springer, Berlin, 2001).
- [46] I. Muller and T. Ruggeri, *Rational Extended Thermodynamics* (Springer, Berlin, 1998).
- [47] B. Derrida, E. Domany, and D. Mukamel, *J. Stat. Phys.* **69**, 667 (1992); B. Derrida, M.R. Evans, V. Hakim, and V. Pasquier, *J. Phys. A* **26**, 1493 (1993).
- [48] B. Derrida, J.L. Lebowitz, and E.R. Speer, *Phys. Rev. Lett.* **87**, 150601 (2001); *J. Stat. Phys.* **107**, 599 (2002).
- [49] G. Schütz, *J. Stat. Phys.* **71**, 471 (1993).
- [50] J. Krug, *Phys. Rev. Lett.* **67**, 1882 (1991).
- [51] M. Hankel and G. Schütz, *Physica A* **206**, 187 (1994).
- [52] A.B. Kolomeisky, G. Schütz, E.B. Kolomeisky, and J.P. Straley, *J. Phys. A* **31**, 6911 (1998).